

Local Perception-Aware Transformer for Aerial Tracking

Changhong Fu^{1,*}, Weiyu Peng¹, Sihang Li¹, Junjie Ye¹, and Ziang Cao²

Abstract—Transformer-based visual object tracking has been utilized extensively. However, the Transformer structure is lack of enough inductive bias. In addition, only focusing on encoding the global feature does harm to modeling local details, which restricts the capability of tracking in aerial robots. Specifically, with local-modeling to global-search mechanism, the proposed tracker replaces the global encoder by a novel local-recognition encoder. In the employed encoder, a local-recognition attention and a local element correction network are carefully designed for reducing the global redundant information interference and increasing local inductive bias. Meanwhile, the latter can model local object details precisely under aerial view through detail-inquiry net. The proposed method achieves competitive accuracy and robustness in several authoritative aerial benchmarks with 316 sequences in total. The proposed tracker’s practicability and efficiency have been validated by the real-world tests. The source code is available at <https://github.com/vision4robotics/LPAT>.

I. INTRODUCTION

Visual object tracking has received more and more attention in the past few decades. It facilitates numerous intelligent applications of robots as a fundamental task, such as obstacle avoidance [1], self location [2], and infrastructure inspection [3]. However, different from general object tracking, the object tracking for aerial robots faces more complicated and difficult challenges, *e.g.*, rotation, deformation and fast motion [4]. Moreover, limited computation resources on aerial robots and requirements for real-time tracking call for a faster and more robust tracker.

The current trackers [5]–[10] adopt ingeniously designed convolutional neural network (CNN) structure to extract local information of correlation feature map effectively. However, the CNNs’ inherent shortage of modeling long-range dependencies weakens the tracker’s capability to search global potential objects under aerial view. Additionally, these recent works need to stack enough layers for expanding the receptive field, which consequently causes large consumption of the computation resource.

To address the shortages of traditional CNN-based trackers, Transformer [11] is introduced into the trackers [12], [13] to increase the capability to model long-range dependencies. Benefiting from gathering global information, they can achieve comparable accuracy when adopting a backbone with fewer layers, compared with the fully CNN-based trackers [14]. However, the typical Transformer adopted

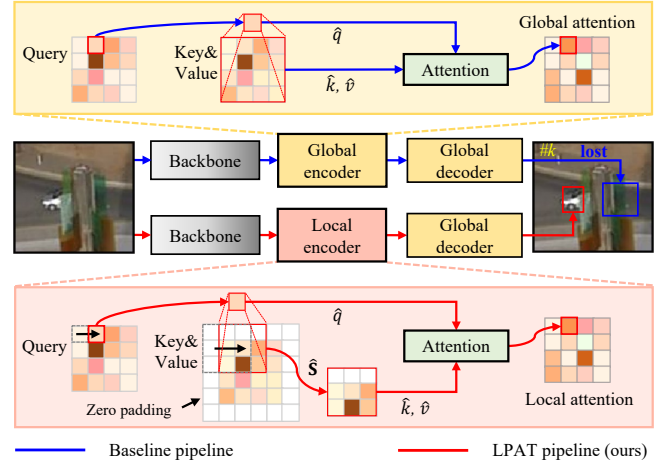


Fig. 1. Comparison of the baseline and LPAT. Local attention is adopted in LPAT to make the tracker focus on local details. The local-to-global architecture exploits the representational ability of Transformer further. \hat{q} denotes a token of the sequence Query. \hat{k} and \hat{v} denote the sequences of Key and Value of the local scope \hat{S} respectively. The proposed tracker with the local inductive bias further gains stronger robustness.

in recent works [12]–[14] lacks intrinsic inductive bias to deal with objects at various scales in modeling local visual structures like CNNs. Under this limitation, the Transformer encoder in a Transformer-based tracker introduces background interference and cannot effectively model the local details of the object when expanding the receptive field with global attention. To address these problems, a special construction method with more local inductive bias is needed for the Transformer-based tracker which will help capture more local details for tackling challenges, *e.g.*, rotation, deformation and fast motion.

Recent works in other fields have paid attention to the inductive bias limitation and attend to increase it in the Transformer-based structure. DeiT [15] proposes a distilling knowledge training method from CNNs to Transformers, which requires a well-trained CNN model as the teacher to introduces the CNNs’ local inductive bias but consumes extra training costs. ViTAE [16] combines CNNs and multi-head self-attention but lacks sufficient exploration of the overall Transformer structure’s inductive bias. Limiting self-attention into a local region, ViL [17] adopts the overlapped windows as convolutions to process all the tokens, but lacks local finer details modeling.

Addressing the limitations above, this work constructs a novel Transformer-based aerial tracker with a local-to-global mechanism, in which two novel local perception-aware blocks are carefully designed. The two blocks are set in two parallel branches to represent local elements which further enhances the network’s perception of local details.

¹Changhong Fu, Weiyu Peng, Sihang Li and Junjie Ye are with the School of Mechanical Engineering, Tongji University, 201804 Shanghai, China. changhongfu@tongji.edu.cn

²Ziang Cao is with the School of Automotive Studies, Tongji University, 201804 Shanghai, China.

*Corresponding author

As compared with the typical Transformer-based tracker in Fig. 1, the proposed framework exploits the local inductive bias of the Transformer further to cope with extremely complex conditions.

The main contributions of this work are listed below:

- A novel Transformer-based tracker with local-modeling to global-search information processing mechanism is proposed to compensate for detailed feature modeling of the Transformer modules and retain the powerful processing capabilities for global information.
- A local-recognition attention block (LRA) is designed to fuse and encode features efficiently with local receptive field. The proposed attention mechanism introduces the local inductive bias to the attention block and improves the tracker’s capability to capture more local details.
- A local element correction network (LEC) is constructed to compensate for the detailed feature modeling of Transformer. This network can enhance the local representation by fusing multi-scale elements.
- Extensive experiments on the representative benchmarks and real-world tests show the proposed method’s out-performance upon SOTA approaches fairly, which demonstrates LPAT’s efficiency and robustness.

II. RELATED WORKS

A. Trackers for Aerial Object Tracking

Siamese network-based trackers [5]–[10] adopt offline-trained CNNs to extract deep features of both template frame and searching frame and search the best matching region after feature maps correlation, which further exploits the local representation than correlation filter-based trackers [18]–[21]. L. Bertinetto *et al.* [7] propose the first model which incorporates feature correlation into a Siamese framework. B. Li *et al.* [8] combines a Siamese network with region proposal networks for more efficient classification and more accurate bounding boxes prediction. SiamCAR [9] achieves a precise performance with a simple anchor-free framework. SiamRTU [10] not only crafts a location module subnetwork for locating the target, but also explores the application of various model update mechanisms. SiamAPN [22] exploits the anchor-free network further in Unmanned Aerial Vehicle (UAV) tracking task and gains promising performances on several typical benchmarks. Naturally, local pixels are more likely to be correlated in images, which suggests that CNNs have an inductive bias in modeling local dependencies. However, trackers with fully CNN-based architecture have to adopt a deeper network and face the limitation in efficient long-range dependencies modeling. Such inductive bias in CNN is not sufficient but important for Transformer-based aerial tracking. This work introduces the CNN-like inductive bias to a Transformer-based tracker by cross-module local-to-global mechanism and precise local details modeling.

B. Transformer Tracking

Transformer was first introduced by A. Vaswani *et al.* [11] and applied in machine translation and is recently introduced

into the domain of computer vision. Vision Transformer has been proven its efficiency in various vision tasks [23]–[26]. Especially in the field of object tracking, Transformer-based trackers with global attention blocks demonstrate their powerful global dependencies modeling capabilities. TransT [27] achieves promising accuracy by replacing the standard correlation layer with cross-attention Transformer block. STARK [13] gathers the global space and temporal information for end-to-end regression and classification, and experiments illustrate its preferable performance. To design a Transformer tracker for aerial platforms, HiFT [14] proposes a lightweight Transformer architecture to fuse features and validate its method’s efficiency in real-world tests. TC-Track [28] exploits the temporal prior knowledge further for both feature extraction and similarity map refinement. However the current Transformer trackers all adopt the typical Transformer structures which is limited in modeling local details, and it is not enough when trackers only learn the inductive bias from data implicitly.

C. Inductive Bias of Transformer

Achieving promising results in vision tasks, inductive biases of the typical Transformer are exploited further. Aiming to reduce the number of datasets and speed up training, DeiT [15] adopts knowledge distillation from CNNs to Transformers, which facilitates the training of vision Transformers by introducing the inductive bias from CNNs. On the other hand, the inductive biases required for the vision task cannot all be learned from training. Recently, some works [17], [29], [30], introduce the intrinsic inductive bias like CNNs into the attention of Transformer directly. To exploit the locality and global dependencies further, ViTAE [16] achieves effective representation by stacking convolutions and attention layers sequentially. Regrettably, the task-required inductive bias of Transformer is becoming an important direction in several vision tasks but not further exploited in aerial object tracking. This work firstly attempts to systematically augment the Transformer’s local inductive bias to exploit cross-module local-to-global mechanism for aerial object tracking.

III. METHODOLOGY

The presented method shown in Fig. 2 is constructed with a weight-shared backbone to extract features, a Transformer module to process features, and a prediction head to predict the location of the object.

A. Local-Recognition Attention

In order to eliminate background interference and introduce the local inductive bias, this work proposes a novel local-recognition attention block. Different from the attention of typical Transformer modules, LRA adopts the local receptive field to eliminate background interference and reduce the time and space complexity to $O(n)$. Convolution layers for embedding queries and keys are deployed to explore the inductive bias of attention structure, and the linear layer for embedding values is kept to maintain tokens’ independence.

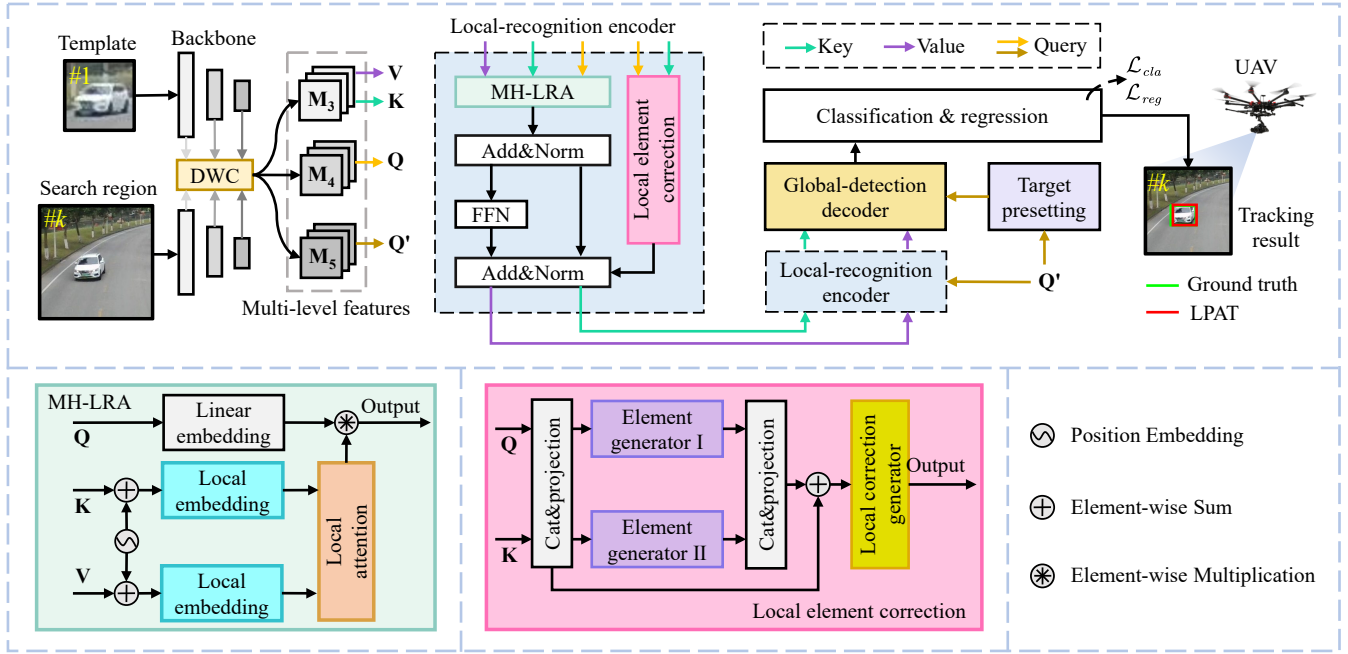


Fig. 2. The proposed framework. Sub-graphs illustrate the specific structure of the modules corresponding to the colors respectively. DWC denotes the deep-wised correlation layer. MH-LRA denotes the multi-head local-recognition attention block. FFN is denoted as the feed-forward network. Each block is followed by a normalization layer. Template image and Searching image are input to the weight-shared backbone. The output feature maps of the last three layers operate DWC in pairs and reshape to 3 sequences of tokens, *i.e.*, $\mathbf{M}_3, \mathbf{M}_4, \mathbf{M}_5$. $\mathbf{Q}, \mathbf{K}, \mathbf{V}$ and \mathbf{Q}' represent the different input variables for whole Transformer framework. Each encoder layer is adopted to fuse features at different depths. Through Transformer decoder and CNN prediction head, the final result is selected by the regression scores. (Best viewed in color)

The typical Transformer is built upon the idea of multi-head attention [24] (MHA), which constructs powerful representations at different positions from different subspaces. The standard attention is $O(n^2)$ in time and space complexity due to the requirement to multiply two $n \times d$ matrices. Actually computing the full attention map is expensive and not suitable for local modeling. This work meticulously modifies the Transformer encoder with local-recognition attention to fuse features by setting $k \times k$ local view around every query of \mathbf{Q} . Specifically, $d = c/h$, h is set as the number of parallel attention heads. Then LRA of each head is defined as:

$$\begin{aligned} \hat{h}_j &= \text{LRA}_j(\mathbf{Q}, \mathbf{K}, \mathbf{V}) = \hat{\mathbf{P}}\hat{\mathbf{V}} = \mathcal{G}(\hat{\mathbf{Q}}, \hat{\mathbf{K}})\hat{\mathbf{V}}, \\ \hat{\mathbf{Q}} &= \phi_q(\mathbf{Q}), \hat{\mathbf{K}} = \phi_k(\mathbf{K}), \hat{\mathbf{V}} = \mathbf{V}\mathbf{W}_j^v, \end{aligned} \quad (1)$$

where \hat{h}_j denotes the process pipeline of j -th head. ϕ_q, ϕ_k denote the convolution embedding for \mathbf{Q} and \mathbf{K} respectively, \mathbf{W}_j^v is the matrix for \mathbf{V} 's linear embedding, \mathcal{G} is the proposed local attention function, and $\hat{\mathbf{P}} \in \mathbb{R}^{n \times n}$ is the local attention weight map. Each element of $\hat{\mathbf{P}}$ is defined as:

$$\begin{aligned} \hat{p}_{i,j} &= \frac{e^{\hat{s}_{i,j}}}{\sum_{\hat{g}=1}^n e^{\hat{s}_{i,\hat{g}}}}, \\ \hat{s}_{i,j} &= \begin{cases} \sum_{\hat{l}=1}^{d_m} \hat{q}_{i,\hat{l}} \hat{k}_{j,\hat{l}} & \hat{j} \in \hat{\mathbf{S}}_i \\ -\infty & \hat{j} \notin \hat{\mathbf{S}}_i \end{cases}, \end{aligned} \quad (2)$$

where $\hat{\mathbf{S}}_i$ is the selected local scope refer to position \hat{i} which is defined as Fig. 1, and $\hat{s}_{i,j}, \hat{p}_{i,j}$ represent the element

of score map and \hat{P} respectively. So the multi-head local-recognition attention (MH-LRA) is defined as:

$$\text{MH-LRA}(\mathbf{Q}, \mathbf{K}, \mathbf{V}) = \text{Cat}(\hat{h}_1, \hat{h}_2, \dots, \hat{h}_n)\mathbf{W}^O, \quad (3)$$

where Cat is concatenating tensors in channel dimension, and \mathbf{W}^O is the matrix to project features.

The proposed local-recognition attention is $O(n)$ in time and space complexity and has more inductive bias based on a local receptive field to reduce the distraction of redundant information, which indicates the LRA's efficiency and accuracy on local modeling. The presented Transformer encoder shown in Fig. 2 deploys LRA for powerful local information representation, and builds local-modeling to global-search information process mechanism with standard global attention [11].

B. Local Element Correction Network

To further enhance the Transformer's ability to model local details, the LEC is proposed to guide the network to focus on local details.

LEC adopts networks with different receptive fields to search and refine different low-dimensional details. Consequently a detail-correction map is generated. Specifically, LEC is defined as:

$$\mathbf{T} = \text{LEC}(\mathbf{Q}, \mathbf{K}) = \text{DIN}(\text{Proj}(\text{Cat}(\mathbf{Q}, \mathbf{K}))) \quad (4)$$

where \mathbf{T} is the detail-correction map, Proj layer is adopted to project features to consistent channels, and DIN is the detail-inquire net which is denoted as:

$$\text{DIN}(\mathbf{x}) = \mathbf{x} + \text{Proj}(\text{Cat}(\text{EG}_I(\mathbf{x}), \text{EG}_{II}(\mathbf{x}))) \quad (5)$$

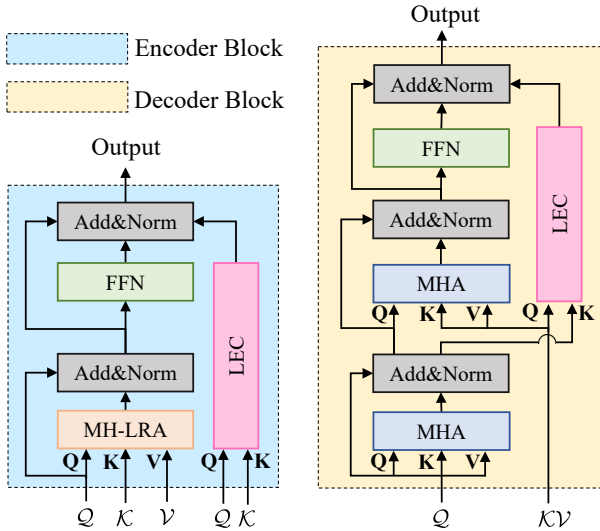


Fig. 3. Left and right represent the proposed Transformer encoder and the standard Transformer decoder respectively. Q , K and V represent the different input variables for an encoder/decoder module. Attributing to the combination of these two structures, LPAT gets the capability of efficient fusion and precise comparative search at the same time.

where EG_* denotes an element generator and \mathbf{x} is the input feature maps.

Remark 1: The branch network is proposed to further increase the local details awareness. For capturing multi-details this work deploys blocks in GoogleNet [31] with different kernel sizes and sets smaller output channel numbers to construct the different element generators.

C. Feature Processing with Local-Global Transformer

Considering the strict requirements for model computational complexity under limited computing resources on aerial robots, LPAT adopts AlexNet [32] to extract features. Both the template branch and the search branch adopt the first five CNN layers of AlexNet as the weight-shared backbone. Specifically, this work denotes the template image and the search image as \mathbf{Z} and \mathbf{X} respectively. The k -th output of the template branch and the search branch are $\varphi_k(\mathbf{Z})$ and $\varphi_k(\mathbf{X})$ respectively.

In order to compare the similarity between the template and search images, feature maps from k -th layer are input to depth-wise cross correlation layer (DWC), and the outputs are reshaped to $\mathbf{M}_k \in \mathbb{R}^{W \times H \times C}$ as:

$$\mathbf{M}_i = \mathcal{F}(\varphi_i(\mathbf{Z}), \varphi_i(\mathbf{X})) , \quad i = 3, 4, 5 \quad (6)$$

where C, W, H represent the channel, width, and height of the feature map respectively, and \mathcal{F} denotes the depth-wise cross correlation layer. Then $\mathbf{M}_3, \mathbf{M}_4, \mathbf{M}_5$ are input to the crafted Transformer module.

1) *Transformer Encoder with Local Attention:* The proposed Transformer encoder adopts LRA for the efficiency of local modeling and LEC as a guide to catch local details. Specifically, as is shown in Fig. 3, each layer of the encoder is constructed with MH-LRA in Eq. (3), LEC, feed-forward network (FFN), and layer normalization (Norm).

Specifically the first encoder module treats \mathbf{M}_3 as \mathbf{K} and \mathbf{V} and \mathbf{M}_4 as \mathbf{Q} to get the first sequence of feature-fused

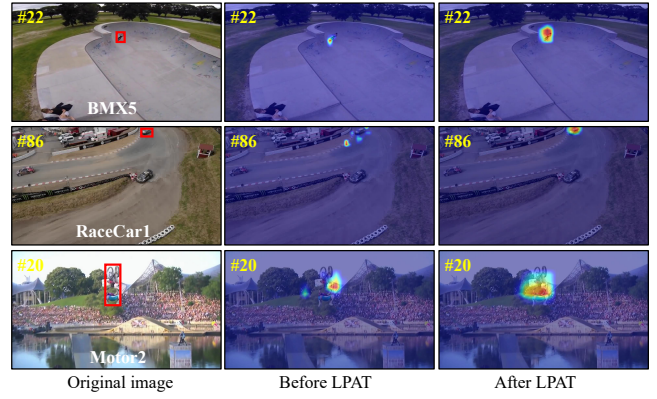


Fig. 4. Visualization of the proposed tracking pipeline. All images are from benchmark DTB70 [33]. Before LPAT, disturbing noises in the search region may affect tracking performance, and LPAT can effectively reduce background interference and focus on the detailed representation of the tracked object to cope with extremely complex situation such as object rotation and deformation.

tokens \mathbf{M}_{E1} , which is denoted as:

$$\begin{aligned} \mathbf{T}_{E1} &= \text{LEC}(\mathbf{M}_3, \mathbf{M}_4) \quad , \\ \hat{\mathbf{M}}_{E1} &= \text{Norm}(\text{MH-LRA}(\mathbf{M}_4, \mathbf{M}_3, \mathbf{M}_3) + \mathbf{M}_4) \quad , \\ \mathbf{M}_{E1} &= \text{Norm}(\mathbf{T}_{E1} + \text{Norm}(\text{FFN}(\hat{\mathbf{M}}_{E1}) + \hat{\mathbf{M}}_{E1})) \quad , \end{aligned} \quad (7)$$

where the $\hat{\mathbf{M}}_{E1}$ is output of first normalization layer of first encoder module, and \mathbf{T}_{E1} is the first detail-correction map.

Remark 2: Compared with the typical Transformer, the proposed local-recognition encoder has powerful representation of local details via LRA and LEC, which keeps the tracker robust in object's appearance change.

Then, the second encoder layer inputs \mathbf{M}_{E1} as \mathbf{K} and \mathbf{V} and \mathbf{M}_5 as \mathbf{Q} , which is denoted as:

$$\begin{aligned} \mathbf{T}_{E2} &= \text{LEC}(\mathbf{M}_{E1}, \mathbf{M}_{E1}) \quad , \\ \hat{\mathbf{M}}_{E2} &= \text{Norm}(\text{MH-LRA}(\mathbf{M}_5, \hat{\mathbf{M}}_{E1}, \hat{\mathbf{M}}_{E1}) + \mathbf{M}_4) \quad , \\ \mathbf{M}_{E2} &= \text{Norm}(\mathbf{T}_{E2} + \text{Norm}(\text{FFN}(\hat{\mathbf{M}}_{E2}) + \hat{\mathbf{M}}_{E2})) \quad , \end{aligned} \quad (8)$$

where $\hat{\mathbf{M}}_{E2}$ is the output of first normalization layer in second encoder module, and \mathbf{T}_{E2} is the second detail-correction map.

Remark 3: In order to effectively fuse multi-scale information, LPAT uses two encoders to achieve a multi-level representation of deep features and shallow features to strengthen the modeling of local details.

2) *Transformer Decoder with Global Attention:* The proposed Transformer decoder adopts global attention for global search. Specifically, as is shown in Fig. 3 each layer of the decoder is constructed with MHA, LEC, FFN, and Norm.

The proposed method adopts DIN to preset the initial tokens of target queries for its rich semantic information, and then treats the final output tokens of encoder, $\hat{\mathbf{M}}_{E2}$, as \mathbf{K}, \mathbf{V} . A LEC layer is also used to guide global-search Transformer to catch local details. The decoder' output sequences (\mathbf{M}_D)

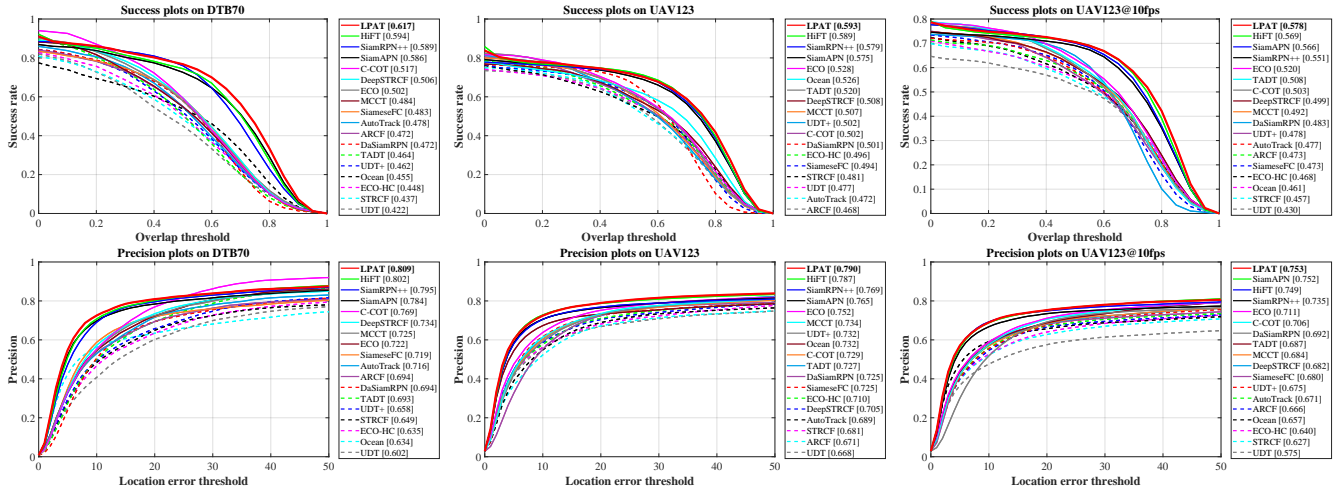


Fig. 5. PPs and SPs of the proposed method and other involved SOTA trackers on authoritative benchmarks, *i.e.*, DTB70, UAV123, and UAV123@10fps. The results indicate the large improvement of LPAT.

is denoted as:

$$\begin{aligned}
 \hat{\mathbf{Q}}_D &= \text{Norm}(\text{MHSA}(\text{DIN}(\mathbf{M}_5))) , \\
 \mathbf{T}_D &= \text{LEC}(\hat{\mathbf{Q}}_D, \hat{\mathbf{M}}_{E2}) , \\
 \hat{\mathbf{M}}_D &= \text{Norm}(\text{MHA}(\hat{\mathbf{Q}}_D, \hat{\mathbf{M}}_{E2}, \hat{\mathbf{M}}_{E2}) + \hat{\mathbf{Q}}_D) , \\
 \mathbf{M}_D &= \text{Norm}(\mathbf{T}_D + \text{Norm}(\text{FFN}(\hat{\mathbf{M}}_D) + \hat{\mathbf{M}}_D)) ,
 \end{aligned} \tag{9}$$

where $\hat{\mathbf{Q}}_D$, \mathbf{T}_D , $\hat{\mathbf{M}}_D$ is the output of the multi-head self-attention layer (MHSA), the cross attention layer and LEC respectively. The visualization of the proposed track pipeline is reported in Fig. 4. Sophisticated local modeling and efficient global search improve the LPAT’s robustness.

Remark 4: The proposed local-global mechanism is built by a cross-module construction method, instead of in-layer feature procession [30], which makes LPAT more robust.

D. Classification & Regression

This work adopts two classification branches and one regression branch [14] which are all constructed by CNN. The cross-entropy loss (\mathcal{L}_{cls1}) is applied to the first classification branch for classification via ground truth area. The binary cross-entropy loss (\mathcal{L}_{cls2}) is applied to the other branch to explore area near the ground truth center point. The regression branch is supervised by IOU loss (\mathcal{L}_{reg}). Therefore, setting λ_* as the hyper-parameter of each different loss, this work determines the overall loss function as:

$$\mathcal{L} = \lambda_1 \mathcal{L}_{cls1} + \lambda_2 \mathcal{L}_{cls2} + \lambda_3 \mathcal{L}_{reg} . \tag{10}$$

IV. EXPERIMENTS

A. Experimental Setup

Evaluation Methodology: In this work, an one-pass evaluation protocol is deployed to evaluate all trackers’ performances via two metrics of success rate and precision [34]. The percentage of frames where the center location error (CLE) is within a given threshold, is demonstrated by the precision. The percentage of frames where the overlap exceeds a given threshold, is visualized via the success rate.

Implementation Details: Image pairs extracted from ImageNet VID [35], COCO [36], GOT-10K [37] and YoutubeBB [38] are used to train the tracker. The sizes of the search region patch and template patch are 287×287 and 127×127 , respectively. The proposed framework adopts the modified AlexNet [32] pretrained with ImageNet [35] as described in SiamRPN [8]. Specifically, the whole network is totally trained for 70 epochs and this work fine-tunes the last three layers of the AlexNet in the last 60 epochs. The learning rate of the back-end networks is initiated as 5×10^{-4} and decreases in the log space from 10^{-2} to 10^{-4} . The training process adopts the stochastic gradient descent (SGD). Additionally, the decay settings of batch size, momentum, and weight are 220, 0.9, and 10^{-4} , respectively. The hardware configuration of the PC deployed to train the network is two NVIDIA TITAN RTX GPUs, an Intel i9-9920X CPU and 32GB RAM. All trackers in this section are evaluated with one NVIDIA TITAN RTX GPU. Our source code and some demo videos are available at <https://github.com/vision4robotics/LPAT>.

B. Overall Performance

The proposed methods are compared with the state-of-the-art trackers including HiFT [14], SiamRPN++ [5], SiamAPN [22], DaSiamRPN [39], C-COT [40], DeepSTRCF [21], ECO [41], ECO-HC [41], Ocean [42], UDT+ [43], SiameseFC [44], ARCF [19], AutoTrack [18], TADT [45] and MCCT [20]. For fairness, a same backbone, *i.e.*, AlexNet pretrained on ImageNet [35] is adopted in all involved Siamese network-based trackers. The detailed comparison results on UAV123 [34], UAV123@10fps [34], and DTB70 [33] benchmarks are reported.

DTB70 [33]: Containing 70 challenging UAV sequences with various extremely complex scenarios, DTB70 is a typical benchmark to evaluate the tracks’ performance. Specifically, the numerous challenges in each sequence include deformation, in-plane rotation, scale variation, *etc.* As presented in the first column of Fig. 5, the proposed tracker gains the best success rate (**0.617**), outperforming the second-

TABLE I

ATTRIBUTE-BASED SUCCESS EVALUATION ON DTB70. **RED**, **GREEN**, AND **BLUE** COLORS ARE ADOPTED TO HIGHLIGHT THE BEST THREE PERFORMANCES IN THE TABLE.

Attr.	Def.	FCM	IPR	MB	OPR	SV
UDT	0.407	0.434	0.389	0.385	0.326	0.464
STRCF	0.390	0.467	0.393	0.447	0.257	0.417
ECO-HC	0.389	0.464	0.401	0.426	0.311	0.429
Ocean	0.371	0.492	0.412	0.409	0.394	0.355
UDT+	0.386	0.476	0.420	0.447	0.289	0.425
TADT	0.449	0.466	0.433	0.450	0.407	0.454
DaSiamRPN	0.493	0.457	0.435	0.404	0.416	0.531
ARCF	0.426	0.496	0.429	0.453	0.321	0.487
AutoTrack	0.452	0.496	0.454	0.468	0.343	0.493
SiameseFC	0.467	0.487	0.447	0.453	0.367	0.483
MCCT	0.466	0.494	0.448	0.478	0.364	0.510
ECO	0.424	0.514	0.451	0.496	0.314	0.481
DeepSTRCF	0.496	0.516	0.475	0.477	0.374	0.518
C-COT	0.430	0.551	0.477	0.522	0.356	0.479
SiamRPN++	0.579	0.587	0.566	0.531	0.484	0.637
SiamAPN	0.616	0.599	0.572	0.525	0.518	0.667
HiFT	0.626	0.611	0.613	0.589	0.546	0.649
LPAT	0.640	0.620	0.623	0.595	0.550	0.670

best HiFT (0.594) and the third-best SiamRPN++ (0.589) by **3.87%** and **4.75%**. Meanwhile, in the precision, LPAT also surpasses others with the best precision **0.809**, while the second-best HiFT and the third-best SiamRPN++ gain 0.802 and 0.795 respectively.

UAV123@30fps [34]: Consisting of 123 sequences with more than 112K frames, the benchmark is adopted to evaluate the performances in a low-altitude aerial perspective. In this benchmark, trackers are facing the numerous challenging scenarios in aerial tracking, *e.g.* scale variation and fast motion. As illustrated in the third column of Fig. 5, LPAT outperforms others in success rate and achieves the best performance with **0.593** success rate and **0.790** precision.

UAV123@10fps [34]: Sequences in this benchmark are downsampled from those recorded in 30 fps. Consequently, the attribute of object motion in UAV123@10fps is more severe and challenging, which is reported in the third column of Fig. 5. LPAT outperforms other trackers with **0.578** success rate and **0.753** precision.

The higher performances on the above benchmarks indicate the accuracy and robustness of LPAT, which shows the powerful local modeling and effective global searching.

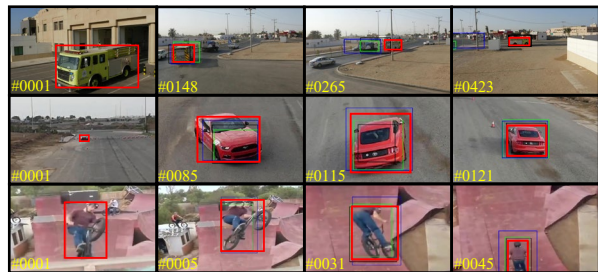
C. Attribute-based Comparison

The robustness of LPAT under extremely complex challenges is evaluated via attribute-based comparisons in DTB70 [33]. The success rate is adopted to describe the accuracy and robustness. Results of success rates on several extremely complex challenges are reported in TABLE I, including deformation (Def.), fast camera motion (FCM),

TABLE II

ABLATION STUDY FOR THE PROPOSED METHOD. LPAT ACHIEVES THE GREAT PERFORMANCE WITH FULLY METHOD.

Methods	Precision	$\Delta_{pre}(\%)$	Success	$\Delta_{suc}(\%)$
Baseline	0.751	—	0.562	—
LRA	0.799	6.39	0.587	4.45
LRA+LEC	0.792	5.46	0.602	7.12
LRA+LEC+LG (LPAT)	0.809	7.19	0.617	9.78



— Ours — HiFT — SiamRPN++ — SiamAPN

Fig. 6. Screenshots of *truck1* from UAV123@30fps, *car16_1* from UAV123@10fps, and *BXM3* from DTB70. The proposed LPAT performs excellently in extremely complex aerial object tracking scenario.

in-plane rotation (IPR), motion blur (MB), out-of-plane rotation (OPR) and scale variation (SV). The proposed tracker achieves the best scores in most scenarios. Especially in in-plane rotation and deformation, the powerful local details perception-aware framework with meticulous local modeling increases the performance of global search via effective perception for object's multiple variation.

D. Ablation Study

The impact of each block and local-to-global mechanism proposed in this work is analyzed. Baseline is considered as the feature extraction, feature process with global attention-based typical Transformer and the same prediction head. LRA denotes adopting local-recognition attention to replace attention blocks in encoder and processes information by local to local mechanism in baseline. LEC denotes adopting local element correction network for all Transformer blocks. LG denotes adopting local to global information processing method. The success and precision are reported in TABLE II. Compared with Baseline, LPAT is indicated that the proposed blocks, LRA and LEC both can effectively increase the accuracy of the Baseline, and the proposed local-modeling to global-search information processing mechanism is also indispensable for LPAT.

E. Comparison to Trackers with Deeper Backbone

To verify the efficiency, the presented method is compared in DTB70 [33] with other trackers with deeper backbones, *i.e.*, SiamRPN++ (ResNet-50) [5], SiamRPN++ (MobileNetV2) [5], SiamMask (ResNet-50) [48], SiamCAR (ResNet-50) [9], SiamDW_RPN (ResNet-22) [46] and SiamGAT (GoogleNet) [47]. The results are reported in TABLE III. LPAT performs the best on both success rate and precision with AlexNet which only has five layers. This comparison indicates the superior efficiency and performance of the proposed method.

F. Qualitative Evaluations

Some qualitative evaluations are released in Fig. 6. Compared with several state-of-the-art trackers [5], [14], [22], LPAT is able to more appropriately predict bounding box in multiple extremely complex challenges, *e.g.*, partial occlusion, in-plane rotation, fast motion, scale variation and low resolution. It is clearly illustrated that the proposed tracker designed for object tracking maintains superior accuracy and robustness via powerful local perception.

TABLE III

CONTRAST WITH DEEPER BACKBONE-BASED TRACKERS IN DTB70. THE PROPOSED METHOD’S BEST PERFORMANCE BENEFITS FROM THE EFFICIENT TRANSFORMER FRAMEWORK. RED, GREEN, AND BLUE COLORS ARE ADOPTED TO HIGHLIGHT THE BEST THREE PERFORMANCES RESPECTIVELY.

Trackers	SiamRPN++ [5]	SiamDW_RPN [46]	SiamGAT [47]	SiamMASK [48]	SiamCAR [9]	SiamRPN++ [5]	LPAT(ours)
Backbone	MobileNetV2 [49]	ResNet-22 [50]	GoogleNet [31]	ResNet-50 [50]	ResNet-50 [50]	ResNet-50 [50]	AlexNet [32]
Success	0.593	0.453	0.583	0.571	0.597	0.615	0.617
Precision	0.785	0.709	0.752	0.769	0.801	0.802	0.809

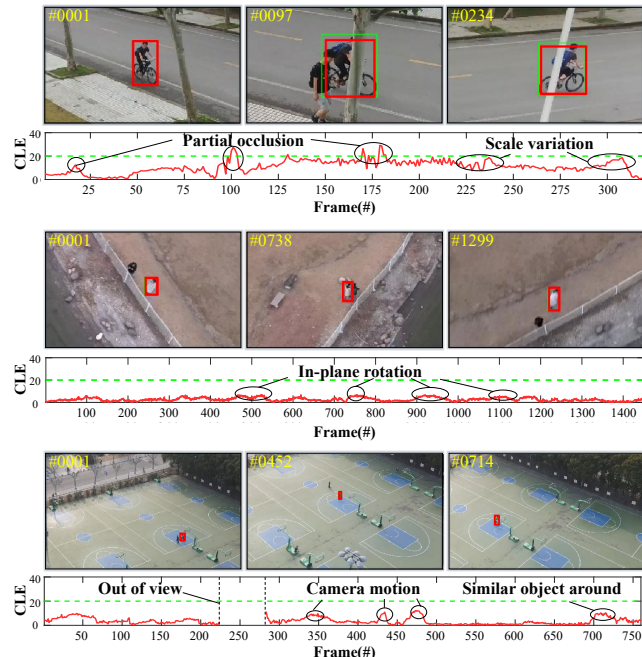


Fig. 7. Real-world tests. The proposed tracker is tested on a common UAV platform with typical embedded processor, *i.e.*, NVIDIA Jetson AGX Xavier. The tracking results and ground truth are marked with red and green box respectively.

V. REAL-WORLD TESTS

Besides the superior performance of LPAT which is shown in Sec. IV, this section reports the LPAT’s capability in real-world scene. The presented tracker is deployed on a common UAV platform with typical embedded processor, *i.e.*, NVIDIA Jetson AGX Xavier. In Fig. 7, the tests’ results are presented. It is noted that the tests face many challenges in complex scenes, especially scale variation, partial occlusion (the first row), in-plane rotation, low-resolution (the second row), out of view, camera motion and small object (the last row). The proposed tracker contrasted with the meticulous local-to-global Transformer framework achieves considerable results in complex actual environments and maintains about 21FPS in the tests. The promising performances indicate the LPAT’s strong robustness in different challenges and the efficiency in aerial application scenarios.

VI. CONCLUSIONS

This work presents a unified framework working in a local-global mechanism to fuse features and directly input to a prediction head for the final tracking result. LRA not only reduces the consumption of computing resources but also suppresses the introduction of interference information. In another parallel pipeline, LEC also improves the Transformer modules’ local details representation abilities. At-

tributing to the efficiency of local-global mechanism, the presented tracker achieves promising performances in different benchmarks and real-world tests with competitive speed. It is convinced that more efficient blocks with the local inductive bias and more delicate local-to-global mechanism will further improve Transformer-based aerial object tracking.

ACKNOWLEDGMENT

This work is supported by the National Natural Science Foundation of China (No. 62173249) and the Natural Science Foundation of Shanghai (No. 20ZR1460100).

REFERENCES

- [1] H. Chen and P. Lu, “Computationally Efficient Obstacle Avoidance Trajectory Planner for UAVs Based on Heuristic Angular Search Method,” in *Proceedings of IEEE/RSJ International Conference on Intelligent Robots and Systems (IROS)*, 2020, pp. 5693–5699.
- [2] J. Ye, C. Fu, F. Lin, F. Ding, S. An, and G. Lu, “Multi-Regularized Correlation Filter for UAV Tracking and Self-Localization,” *IEEE Transactions on Industrial Electronics*, vol. 69, no. 6, pp. 6004–6014, 2022.
- [3] J. Fu, A. Núñez, and B. De Schutter, “Real-Time UAV Routing Strategy for Monitoring and Inspection for Postdisaster Restoration of Distribution Networks,” *IEEE Transactions on Industrial Informatics*, vol. 18, no. 4, pp. 2582–2592, 2022.
- [4] C. Fu, B. Li, F. Ding, F. Lin, and G. Lu, “Correlation Filters for Unmanned Aerial Vehicle-Based Aerial Tracking: A Review and Experimental Evaluation,” *IEEE Geoscience and Remote Sensing Magazine*, vol. 10, no. 1, pp. 125–160, 2022.
- [5] B. Li, W. Wu, Q. Wang, F. Zhang, J. Xing, and J. Yan, “SiamRPN++: Evolution of Siamese Visual Tracking with Very Deep Networks,” in *Proceedings of the IEEE/CVF Conference on Computer Vision and Pattern Recognition (CVPR)*, 2019, pp. 4277–4286.
- [6] Z. Chen, B. Zhong, G. Li, S. Zhang, and R. Ji, “Siamese Box Adaptive Network for Visual Tracking,” in *Proceedings of the IEEE/CVF Conference on Computer Vision and Pattern Recognition (CVPR)*, 2020, pp. 6668–6677.
- [7] L. Bertinetto, J. Valmadre, J. F. Henriques, A. Vedaldi, and P. H. Torr, “Fully-Convolutional Siamese Networks for Object Tracking,” in *Proceedings of the European Conference on Computer Vision (ECCV)*, 2016, pp. 850–865.
- [8] B. Li, J. Yan, W. Wu, Z. Zhu, and X. Hu, “High Performance Visual Tracking with Siamese Region Proposal Network,” in *Proceedings of the IEEE/CVF Conference on Computer Vision and Pattern Recognition (CVPR)*, 2018, pp. 8971–8980.
- [9] D. Guo, J. Wang, Y. Cui, Z. Wang, and S. Chen, “SiamCAR: Siamese Fully Convolutional Classification and Regression for Visual Tracking,” in *Proceedings of the IEEE/CVF Conference on Computer Vision and Pattern Recognition (CVPR)*, 2020, pp. 6269–6277.
- [10] F. Zhao, T. Zhang, Y. Song, M. Tang, X. Wang, and J. Wang, “Siamese Regression Tracking with Reinforced Template Updating,” *IEEE Transactions on Image Processing*, vol. 30, pp. 628–640, 2020.
- [11] A. Vaswani, N. Shazeer, N. Parmar, J. Uszkoreit, L. Jones, A. N. Gomez, Ł. Kaiser, and I. Polosukhin, “Attention Is All You Need,” in *Proceedings of the Advances in Neural Information Processing Systems (NIPS)*, 2017, pp. 6000–6010.
- [12] X. Chen, B. Yan, J. Zhu, D. Wang, X. Yang, and H. Lu, “Transformer Tracking,” in *Proceedings of the IEEE/CVF Conference on Computer Vision and Pattern Recognition (CVPR)*, 2021, pp. 8126–8135.
- [13] B. Yan, H. Peng, J. Fu, D. Wang, and H. Lu, “Learning Spatio-Temporal Transformer for Visual Tracking,” in *Proceedings of the IEEE/CVF International Conference on Computer Vision (ICCV)*, 2021, pp. 10448–10457.

- [14] Z. Cao, C. Fu, J. Ye, B. Li, and Y. Li, "HiFT: Hierarchical Feature Transformer for Aerial Tracking," in *Proceedings of the IEEE/CVF International Conference on Computer Vision (ICCV)*, 2021, pp. 15 457–15 466.
- [15] H. Touvron, M. Cord, M. Douze, F. Massa, A. Sablayrolles, and H. Jégou, "Training Data-efficient Image Transformers & Distillation through Attention," in *Proceedings of the International Conference on Machine Learning (ICML)*, 2021, pp. 10 347–10 357.
- [16] Y. Xu, Q. Zhang, J. Zhang, and D. Tao, "ViTAE: Vision Transformer Advanced by Exploring Intrinsic Inductive Bias," *Advances in Neural Information Processing Systems (NIPS)*, pp. 28 522–28 535, 2021.
- [17] P. Zhang, X. Dai, J. Yang, B. Xiao, L. Yuan, L. Zhang, and J. Gao, "Multi-Scale Vision Longformer: A New Vision Transformer for High-Resolution Image Encoding," in *Proceedings of the IEEE/CVF Conference on Computer Vision and Pattern Recognition (CVPR)*, 2021, pp. 2998–3008.
- [18] Y. Li, C. Fu, F. Ding, Z. Huang, and G. Lu, "AutoTrack: Towards High-Performance Visual Tracking for UAV with Automatic Spatio-Temporal Regularization," in *Proceedings of the IEEE/CVF Conference on Computer Vision and Pattern Recognition (CVPR)*, 2020, pp. 11 923–11 932.
- [19] Z. Huang, C. Fu, Y. Li, F. Lin, and P. Lu, "Learning Aberrance Repressed Correlation Filters for Real-Time UAV Tracking," in *Proceedings of the IEEE/CVF International Conference on Computer Vision (ICCV)*, 2019, pp. 2891–2900.
- [20] N. Wang, W. Zhou, Q. Tian, R. Hong, M. Wang, and H. Li, "Multi-Cue Correlation Filters for Robust Visual Tracking," in *Proceedings of the IEEE/CVF Conference on Computer Vision and Pattern Recognition (CVPR)*, 2018, pp. 4844–4853.
- [21] F. Li, C. Tian, W. Zuo, L. Zhang, and M.-H. Yang, "Learning Spatial-Temporal Regularized Correlation Filters for Visual Tracking," in *Proceedings of the IEEE/CVF Conference on Computer Vision and Pattern Recognition (CVPR)*, 2018, pp. 4904–4913.
- [22] C. Fu, Z. Cao, Y. Li, J. Ye, and C. Feng, "Onboard Real-Time Aerial Tracking with Efficient Siamese Anchor Proposal Network," *IEEE Transactions on Geoscience and Remote Sensing*, vol. 60, pp. 1–13, 2022.
- [23] P. Esser, R. Rombach, and B. Ommer, "Taming Transformers for High-Resolution Image Synthesis," in *Proceedings of the IEEE/CVF Conference on Computer Vision and Pattern Recognition (CVPR)*, 2021, pp. 12 873–12 883.
- [24] A. Dosovitskiy, L. Beyer, A. Kolesnikov, D. Weissenborn, X. Zhai, T. Unterthiner, M. Dehghani, M. Minderer, G. Heigold, S. Gelly *et al.*, "An Image is Worth 16x16 Words: Transformers for Image Recognition at Scale," in *Proceedings of the International Conference on Learning Representations (ICLR)*, 2021, pp. 1–21.
- [25] C.-F. R. Chen, Q. Fan, and R. Panda, "CrossViT: Cross-Attention Multi-Scale Vision Transformer for Image Classification," in *Proceedings of the IEEE/CVF Conference on Computer Vision and Pattern Recognition (CVPR)*, 2021, pp. 357–366.
- [26] S. Zheng, J. Lu, H. Zhao, X. Zhu, Z. Luo, Y. Wang, Y. Fu, J. Feng, T. Xiang, P. H. Torr, and L. Zhang, "Rethinking Semantic Segmentation From a Sequence-to-Sequence Perspective with Transformers," in *Proceedings of the IEEE/CVF Conference on Computer Vision and Pattern Recognition (CVPR)*, 2021, pp. 6881–6890.
- [27] H. Chen, Y. Wang, T. Guo, C. Xu, Y. Deng, Z. Liu, S. Ma, C. Xu, C. Xu, and W. Gao, "Pre-Trained Image Processing Transformer," in *Proceedings of the IEEE/CVF Conference on Computer Vision and Pattern Recognition (CVPR)*, 2021, pp. 12 299–12 310.
- [28] Z. Cao, Z. Huang, L. Pan, S. Zhang, Z. Liu, and C. Fu, "TC-Track: Temporal Contexts for Aerial Tracking," in *Proceedings of the IEEE/CVF Conference on Computer Vision and Pattern Recognition (CVPR)*, 2022, pp. 14 798–14 808.
- [29] Z. Liu, Y. Lin, Y. Cao, H. Hu, Y. Wei, Z. Zhang, S. Lin, and B. Guo, "Swin Transformer: Hierarchical Vision Transformer Using Shifted Windows," in *Proceedings of the IEEE/CVF International Conference on Computer Vision (ICCV)*, 2021, pp. 10 012–10 022.
- [30] X. Chu, Z. Tian, Y. Wang, B. Zhang, H. Ren, X. Wei, H. Xia, and C. Shen, "Twins: Revisiting the Design of Spatial Attention in Vision Transformers," *Advances in Neural Information Processing Systems (NIPS)*, pp. 9355–9366, 2021.
- [31] C. Szegedy, W. Liu, Y. Jia, P. Sermanet, S. Reed, D. Anguelov, D. Erhan, V. Vanhoucke, and A. Rabinovich, "Going Deeper with Convolutions," in *Proceedings of the IEEE/CVF Conference on Computer Vision and Pattern Recognition (CVPR)*, 2015, pp. 1–9.
- [32] A. Krizhevsky, I. Sutskever, and G. E. Hinton, "Imagenet Classification with Deep Convolutional Neural Networks," in *Proceedings of the Advances in Neural Information Processing Systems (NIPS)*, 2012, pp. 1097–1105.
- [33] S. Li and D.-Y. Yeung, "Visual Object Tracking for Unmanned Aerial Vehicles: A Benchmark and New Motion Models," in *Proceedings of the AAAI Conference on Artificial Intelligence*, 2017, pp. 4140–4146.
- [34] M. Mueller, N. Smith, and B. Ghanem, "A Benchmark and Simulator for UAV Tracking," in *Proceedings of the European Conference on Computer Vision (ECCV)*, 2016, pp. 445–461.
- [35] O. Russakovsky, J. Deng, H. Su, J. Krause, S. Satheesh, S. Ma, Z. Huang, A. Karpathy, A. Khosla, M. Bernstein *et al.*, "Imagenet Large Scale Visual Recognition Challenge," *International journal of computer vision*, vol. 115, no. 3, pp. 211–252, 2015.
- [36] T.-Y. Lin, M. Maire, S. Belongie, J. Hays, P. Perona, D. Ramanan, P. Dollár, and C. L. Zitnick, "Microsoft Coco: Common Objects in Context," in *Proceedings of the European Conference on Computer Vision (ECCV)*, 2014, pp. 740–755.
- [37] L. Huang, X. Zhao, and K. Huang, "GOT-10k: A Large High-Diversity Benchmark for Generic Object Tracking in the Wild," *IEEE Transactions on Pattern Analysis and Machine Intelligence*, vol. 43, no. 5, pp. 1562–1577, 2019.
- [38] E. Real, J. Shlens, S. Mazzocchi, X. Pan, and V. Vanhoucke, "Youtube-boundingboxes: A Large High-Precision Human-Annotated Data Set for Object Detection in Video," in *Proceedings of the IEEE/CVF Conference on Computer Vision and Pattern Recognition (CVPR)*, 2017, pp. 5296–5305.
- [39] Z. Zhu, Q. Wang, B. Li, W. Wu, J. Yan, and W. Hu, "Distractor-Aware Siamese Networks for Visual Object Tracking," in *Proceedings of the European Conference on Computer Vision (ECCV)*, 2018, pp. 101–117.
- [40] M. Danelljan, A. Robinson, F. Shahbaz Khan, and M. Felsberg, "Beyond Correlation Filters: Learning Continuous Convolution Operators for Visual Tracking," in *Proceedings of the European Conference on Computer Vision (ECCV)*, 2016, pp. 472–488.
- [41] M. Danelljan, G. Bhat, F. Shahbaz Khan, and M. Felsberg, "ECO: Efficient Convolution Operators for Tracking," in *Proceedings of the IEEE/CVF Conference on Computer Vision and Pattern Recognition (CVPR)*, 2017, pp. 6638–6646.
- [42] Z. Zhang, H. Peng, J. Fu, B. Li, and W. Hu, "Ocean: Object-Aware Anchor-Free Tracking," in *Proceedings of the European Conference on Computer Vision (ECCV)*, 2020, pp. 771–787.
- [43] N. Wang, Y. Song, C. Ma, W. Zhou, W. Liu, and H. Li, "Unsupervised Deep Tracking," in *Proceedings of the IEEE/CVF Conference on Computer Vision and Pattern Recognition (CVPR)*, 2019, pp. 1308–1317.
- [44] L. Bertinetto, J. Valmadre, J. F. Henriques, V. Andrea, and P. H. S. Torr, "Fully-Convolutional Siamese Networks for Object Tracking," in *Proceedings of the European Conference on Computer Vision (ECCV)*, 2016, pp. 850–865.
- [45] X. Li, C. Ma, B. Wu, Z. He, and M.-H. Yang, "Target-Aware Deep Tracking," in *Proceedings of the IEEE/CVF Conference on Computer Vision and Pattern Recognition (CVPR)*, 2019, pp. 1369–1378.
- [46] Z. Zhang and H. Peng, "Deeper and Wider Siamese Networks for Real-Time Visual Tracking," in *Proceedings of the IEEE/CVF Conference on Computer Vision and Pattern Recognition (CVPR)*, 2019, pp. 4591–4600.
- [47] D. Guo, Y. Shao, Y. Cui, Z. Wang, L. Zhang, and C. Shen, "Graph Attention Tracking," in *Proceedings of the IEEE/CVF Conference on Computer Vision and Pattern Recognition (CVPR)*, 2021, pp. 9543–9552.
- [48] Q. Wang, L. Zhang, L. Bertinetto, W. Hu, and P. H. Torr, "Fast Online Object Tracking and Segmentation: A Unifying Approach," in *Proceedings of the IEEE/CVF Conference on Computer Vision and Pattern Recognition (CVPR)*, 2019, pp. 1328–1338.
- [49] M. Sandler, A. Howard, M. Zhu, A. Zhmoginov, and L.-C. Chen, "MobileNetV2: Inverted Residuals and Linear Bottlenecks," in *Proceedings of the IEEE/CVF Conference on Computer Vision and Pattern Recognition (CVPR)*, 2018, pp. 4510–4520.
- [50] K. He, X. Zhang, S. Ren, and J. Sun, "Deep Residual Learning for Image Recognition," in *Proceedings of the IEEE/CVF Conference on Computer Vision and Pattern Recognition (CVPR)*, 2016, pp. 770–778.